# Study on Quality of Pair Distribution Function for Direct Space Approach of Structure Investigation

*A. F. Mabied*[1,2,*], *A. R. Shalaby*[3], *A. A. Ramadan*[4], *M. R. Abaid*[5] *and H. M. Hashem*[4]

[1]Solid State Physics Department, National Research Centre, Dokki, Giza, Egypt
[2]Faculty of Basic Science, King Salman International University (KSIU), Ras Sudr, South Sinai, Egypt
[3]Department of Basic Sciences, October High Institute of Engineering & Technology - OHI, 6th of October, Giza, Egypt
[4]Physics Department, Faculty of Science, Helwan University, Cairo, Egypt
[5]Physics Department, Faculty of Science, Minia University, Minia, Egypt

**Abstract:** Study of the structure characteristics of solid materials is a key for development of technological applications. Potential of direct space approach for structure determination and refinement using powder X-ray diffraction data depend on the quality of pair distribution function (PDF) plot. So, the effect of data collection conditions and diffractogram characteristics on the quality of PDF plot has been investigated in detail. In addition, errors and possible tolerance have been estimated. Some parameters affect only either the X-ray diffractogram or PDF plots and others affect both. Considering the errors and tolerance, direct space approach can be confidently used for structure refinement, where the error did not exceed 10.0 % for inter-atomic radial distance longer than ≈ 2.0 Å and 5.0 % for longer than ≈ 4.0 Å, which is accepted for structure refinement. As tolerance is considered, every time the value of the lattice parameter is changed to smaller or larger than the correct value (± 8.0 %), it comes back to the initial correct one. Although, advanced synchrotron radiation shows better data, conventional source can be used successfully for structure investigation applying direct space approach.

**Keywords:** X-ray diffraction, Pair distribution function, Direct space approach, Structure refinement.

## 1 Introduction

Discovery and development of new and advanced materials are based on the correlation between their functional physical and chemical properties and their structure in long and short range of atomic scale [1]. For crystalline materials X-ray powder diffraction is used to determine the atomic-scale structure of materials [2] which is a fundamental material property that specifies how atoms are arranged in space. In the classical data analysis (reciprocal space approach), each Bragg peak is isolated. However, if the structure is not perfectly periodic, due to dynamic or static local deviations, the limitations of the crystallographic methods become apparent [1]. Thus, classical analysis limits the use of powder diffraction in crystal structure investigations, when the Bragg peaks get closer together and start to overlap each other [3].

One of the most challenging problems in the study of structure is to characterize the atomic short-range order such as nanocrystalline or amorphous materials. Using PDF method for investigation of polycrystalline and amorphous materials in the form of powder or thin films serves strongly in both the short as well as the long range atomic scale, which has a significant and clear impact on the applications in various fields of technology [4,5]. Such atomic scale structure for materials of limited structural coherence is characterized by Pair distribution function, PDF, analysis of direct space approach [6]. This technique was first applied on liquids and glasses [7]. Now, it is extended to crystalline materials with intrinsic disorder and nanosized grains [8,9]. The degree of structural coherence in condensed materials from crystalline solid to liquid or something in between can be easily recognized by examining the PDF plot [8].

Limit, potential and capability of direct space approach for structure investigation (determination or refinement) using powder X-ray diffraction data depend on the pair distribution function (PDF). Thus, the effect of data collection conditions and diffractogram characteristics on the quality of PDF plot has to be investigated individually and in detail. In addition, errors and possible tolerance have to be estimated. Simulated data of a compound of known crystal structure will be used to verify the pair distribution

*Corresponding author E-mail: ahmed730102@yahoo.com

function. Different experimental (data collection) parameters as well as diffraction patterns characteristics will be considered. Both the conventional X-ray source as well as the advanced Synchrotron radiation will be considered [6,8,10].

## 2 Computational Works:

Powder Cell for Windows was used for exploring crystal structures and calculating powder patterns [11]. Rietveld refinement and data visualization were performed through FULLPROF Suit [12] and MAUD software [13]. RAD is an interactive computer program for radial distribution analysis of X-ray diffraction data [14], as well as PDFgetX3 were used for converting X-ray powder diffraction data to an atomic pair distribution function (PDF) [10]. Peak Fitting Program (Fityk) was used for nonlinear curve fitting and data analysis [15]. Real-space refinement of crystal structures based on the atomic pair distribution function method was carried out by PDFgui program, which can also simplifies many data analysis tasks [16].

## 3 Results and Discussion:

### 3.1 Pair Distribution Function Determination (PDF)

In order to compare the direct and reciprocal space approaches for crystal structure determination or refinement using powder X-ray diffraction data, the first step is to get a correct and representative pair distribution function (PDF). Thus, the effect of data collection conditions and diffractogram characteristics on the quality of PDF plot has been verified and individually investigated. In addition, the potential of the used PDFgui program to get the correct refined crystallographic characteristics has been verified and investigated. So that, the errors in the estimated inter-atomic distances from PDF plot compared with those from the simulated ones has been calculated. Also, the possible tolerance to refine one of the structure characteristics (lattice parameter) has been investigated. The compound that was used as reference is $SrTiO_3$ and their structure information [17].

The verified and investigated parameters are:
- Data collection conditions:
  - i- Wavelength, λ, in conventional and advanced synchrotron radiation ranges, at fixed wave vector, $Q_{max}$.
  - ii- Wave vector, $Q_{max}$, at fixed wavelengths, λ.
  - iii- Step size, Δ2θ, at fixed wavelengths, λ, and wave vector, $Q_{max}$.

- Diffractogram characteristic at fixed wavelength, λ, and wave vector, $Q_{max}$:

  - i- Diffraction Peak profile (broadening, FWHM).
    - (a) Instrumental condition.
    - (b) Crystallite size.
    - (c) Internal residual strain.
  - ii- Diffraction intensity (number of counts).

- Crystallographic characteristics:
  - i- Inter-atomic distances (errors).
  - ii- Lattice parameters (tolerance).

### 3.1.1 Data Collection Conditions

**i- Wavelength, λ, at Fixed $Q_{max}$:**

The values of the considered wavelengths in conventional as well as synchrotron radiation ranges are given in Table (1) and the corresponding diffraction patterns are depicted in Figure (1). Since $Q_{max}$ ($4\pi \sin\theta/\lambda$) is kept fixed, the 2θ-range should be changed as the wavelength λ changes. Considering longer wavelength λ, the corresponding 2θ-range increases, so the resolution of the diffraction peaks improves as shown in Figure (1). On the other hand, the peak intensities decrease as the atomic scattering factor (f) decreases considerably as sinθ increases. Thus, from the point of view of diffractogram quality, one has to choose depending on the requirement.

Using PDFgetX3 program, the corresponding PDF calculated from the above diffraction patterns are depicted in Figure (2). The wavelength has a pronounced effect on the quality of PDF plot. In general, as the wavelength become shorter, peaks of the PDF become sharper and of higher intensity s clearly shown in the zoom part (r =1-15Å) of Figure (2). Since the aim is the PDF determination with high quality, short wavelength is recommended.

**Table 1:** Used wavelengths at fixed $Q_{max}$.

| $Q_{max}$ (Å$^{-1}$) | Radiation | | 2θ Range (degree) | |
|---|---|---|---|---|
| | Type | λ (Å) | Min. | Max. |
| 7.00 | Synchrotron | 0.20 | 1.0 | 12.8 |
| | | 0.30 | | 19.5 |
| | | 0.40 | | 26.4 |
| | Conventional | 0.56 (Si- K$_\alpha$) | 2.0 | 39.0 |
| | | 0.71 (Mo-K$_\alpha$) | | 52.0 |
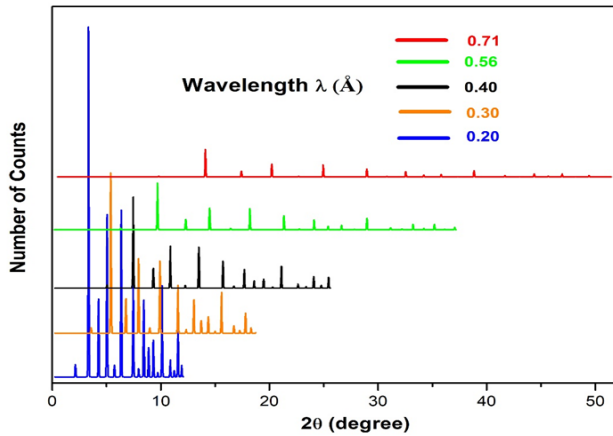
**Fig.1:** Effect of wavelength on XRD patterns.
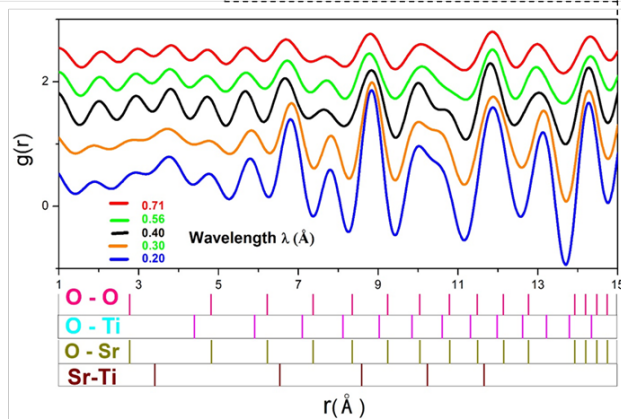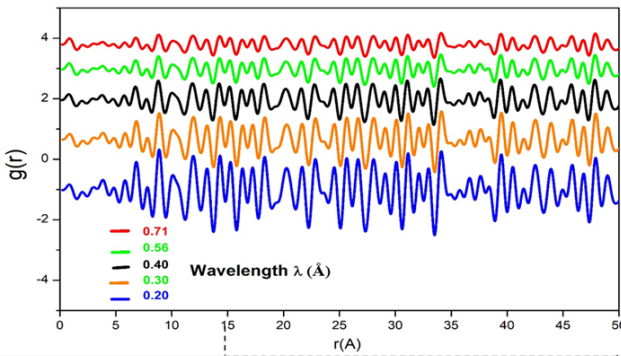


**Fig.2:** Effect of wavelength on: PDF plots.

### ii- Average vector, $Q_{max}$, at fixed Wavelength, λ:

The values of the considered wave vectors and the corresponding 2θ-range are given in Table (2) and the simulated diffraction patterns are depicted in Figures (3a) and (3b) for synchrotron and conventional range, respectively. Since the wavelength is fixed in every group and only the 2θ-range is varied, diffraction patterns of the same quality are obtained but only the number of diffraction peaks increases as the 2θ-range increases. On the other hand, the quality of PDF depicted in Figures (4) and (5) is considerably varies. As the 2θ-range increase and

consequently the number of the diffraction peaks, the PDF beaks become sharp and of higher intensity. This improvement is due to the greater information that are included in the diffraction patterns. So, high $Q_{max}$ is recommended from the point of views of the quality of PDF plot.

**Table 2:** Used values of wave vectors, $Q_{max}$, at fixed wavelengths.

| λ (Å) | $Q_{max}$ (Å$^{-1}$) | 2θ Range (degree) | |
|---|---|---|---|
| | | Min. | Max. |
| 0.3 (Synchrotron) | 7.27 | 1.0 | 20 |
| | 10.84 | | 30 |
| | 14.30 | | 40 |
| 0.56 (Conventional) | 14.4 | 2.0 | 80 |
| | 18.4 | | 110 |
| | 21.1 | | 140 |
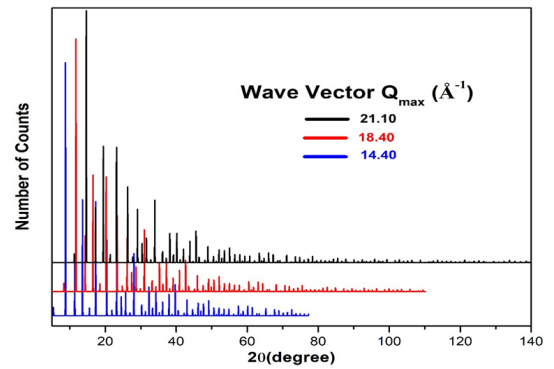


**Fig.3:** Effect of $Q_{max}$ on XRD patterns considering:

(a) synchrotron source and (b) conventional source.

### iii- Step size (Δ2θ):

The values of the considered step size and the corresponding 2θ-range are given in Table (3). The simulated diffraction patterns and zoom on the 100% diffraction peak are depicted in Figure (6a, b). Generally, there is no observed effect on the diffractograms. However, zoom on the 100% diffraction peak shows that the peak maximum is shifted from the correct position as the step size increases and position is defined accurately as Δ2θ decreases. On the other hand, step size change does not affect the PDF plot as it is depicted in Figure (7). So, that, it

is recommended from the point of view of XRD diffractogram quality to decrease the step size to get the accurate position of the diffraction peak.





**Fig.4:** Effect of wave vector on PDF plots considering conventional source.





**Fig.5:** Effect of wave vector on PDF plots considering conventional source.

## 3.1.2 Diffractogram Characteristics at Fixed Wavelength and Wave Vector:

**i- Diffraction peak profile (Broadening, FWHM):**

The FWHM of the Gaussian and Lorentzian components of the function used is specified used in Fullprof program using the following expressions:

FWHM^2 (Gaussian) = ( U + (STR)^2 ∗ Tan^2 θ + V ∗ Tan θ + W + IG/(cos^2 θ))

FWHM (Lorentzian) = X ∗ Tan θ + (Y + (SZ))/(cos Θ)

Crystallite size for both Gaussian and Lorentzian distribution is defined as:

Crystallite size (Gaussian) = 180 λ/π sqrt (IG)

and

Crystallite size (Lorentzian) = 180 λ / π (Y)

where U, V and W are refinable parameters and W represent the effect that not related to either crystallite size nor internal strain.

**(a) Instrumental:**

The values of the considered profile parameters at fixed wavelength and $Q_{max}$ are given in Table (4) and the corresponding diffraction patterns are depicted in Figure (8). It is clear that there is no shift in peak positions. However, diffraction peak width (FWHM) is varied in accordance with the used W profile parameter. As breadth increases, the beak maximum is decreased and the resolution is lost. Thus, the diffractogram deteriorates as FWHM increases. So, it is strongly recommended from the point of view of X-ray diffractogram quality that experimental conditions, which result in sharp diffraction peaks, such as slit width, to be used as possible.
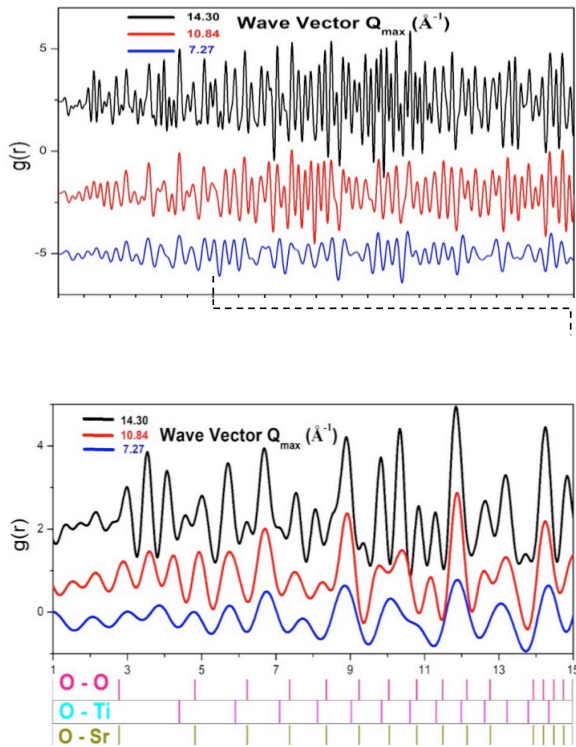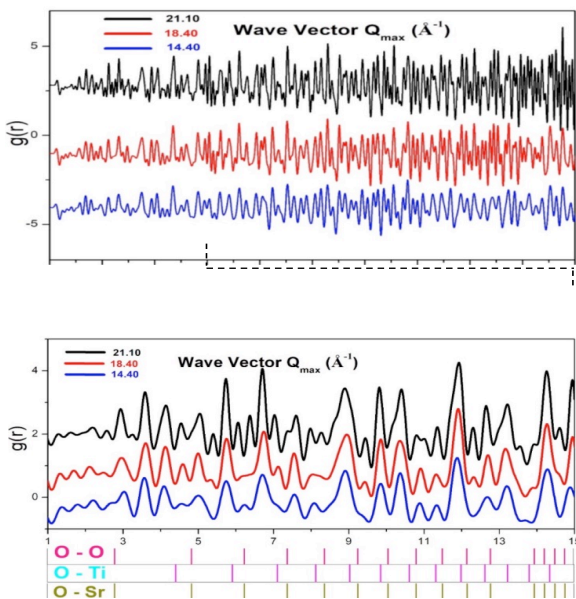
**Table 3:** Used values of step size at fixed $Q_{max}$:

| λ (Å) | $Q_{max}$ (Å$^{-1}$) | 2θ Range (degree) | Step size (Δ2θ) |
|-------|----------|-------------------|-----------------|
| 0.3   | 7.0      | 4.0 - 20.0        | 0.005           |
|       |          |                   | 0.010           |

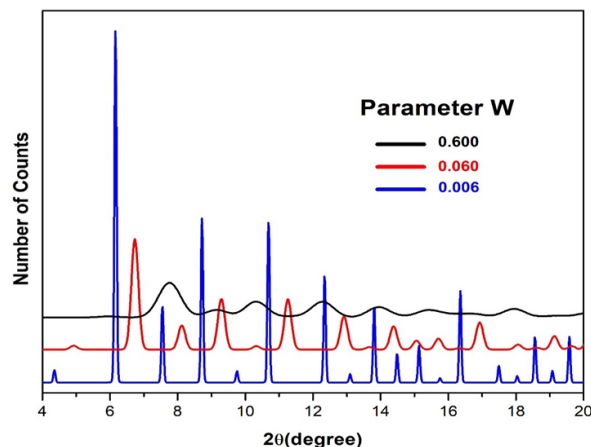**Table 4:** Used values of instrumental parameter (W) at fixed wavelength and wave vector:

| λ (Å) | $Q_{max}$ (Å$^{-1}$) | Shape Parameters | | |
|-------|----------|-------|-------|-------|
|       |          | (u)   | (v)   | (w)   |
| 0.3   | 0.7      | 0.004 | 0.007 | 0.006 |
|       |          |       |       | 0.060 |
|       |          |       |       | 0.600 |
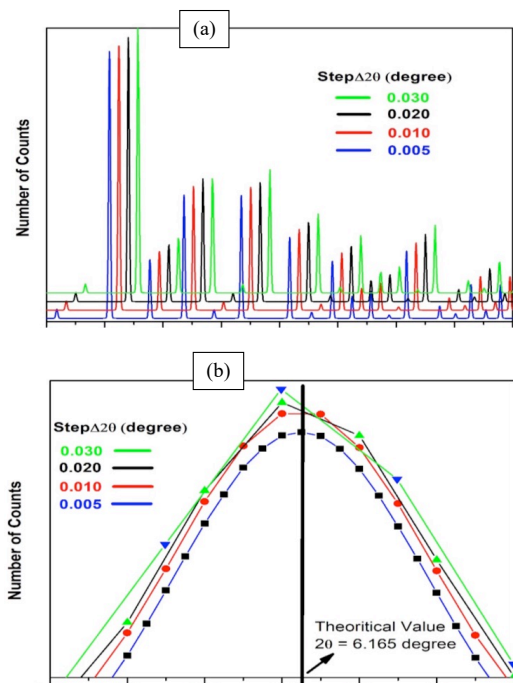
**Fig.6:** Effect of step size at constant wavelength and Qmax on:
(a) Diffraction pattern and (b) 100% peak position.
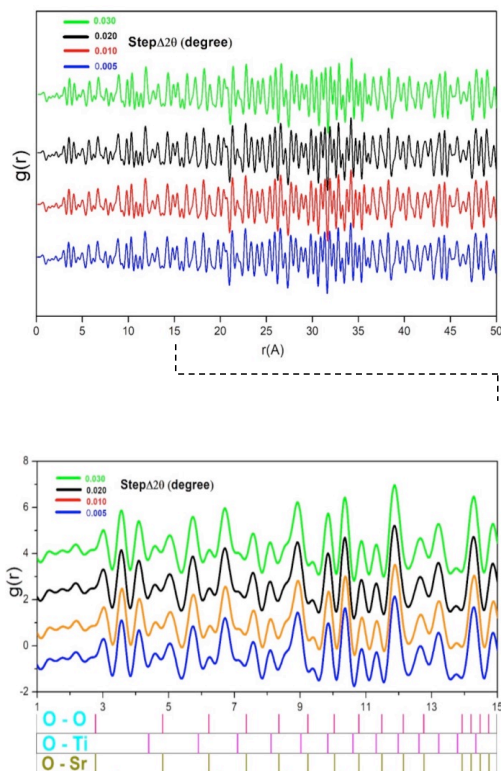


**Fig.7:** Effect step size on PDF plots.



**Fig.8:** Effect of instrumental parameter on X-ray diffractograms.

The obtained PDF plots are depicted in Figure (9). However, the peak heights decrease rapidly and disappear at smaller r-value ($\approx 2.5$Å) as the instrumental broadening increases. However, the peak heights increase the resolution is improved. So that, from the point of view of the quality of PDF plot, experimental conditions, which result in broad diffraction peaks improve the quality in the useful rang up to r = 25Å. Therefore, it is recommended that the experimental conditions used for data collection should be specified for large beak broadening.
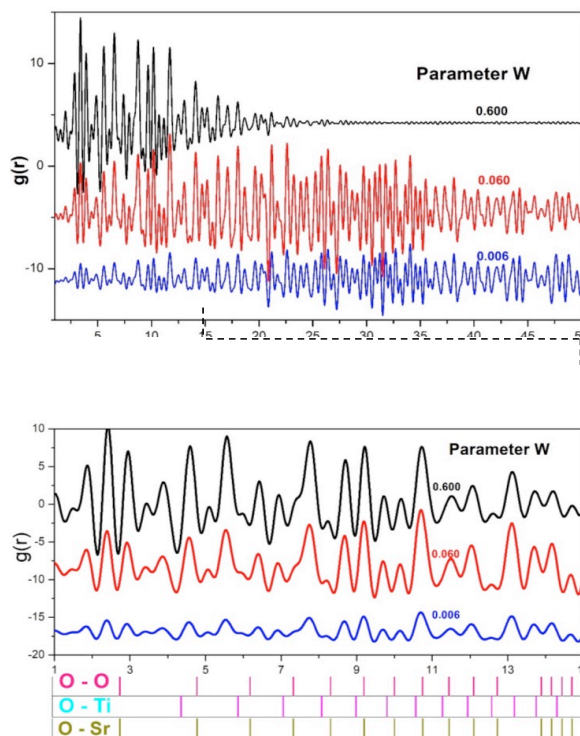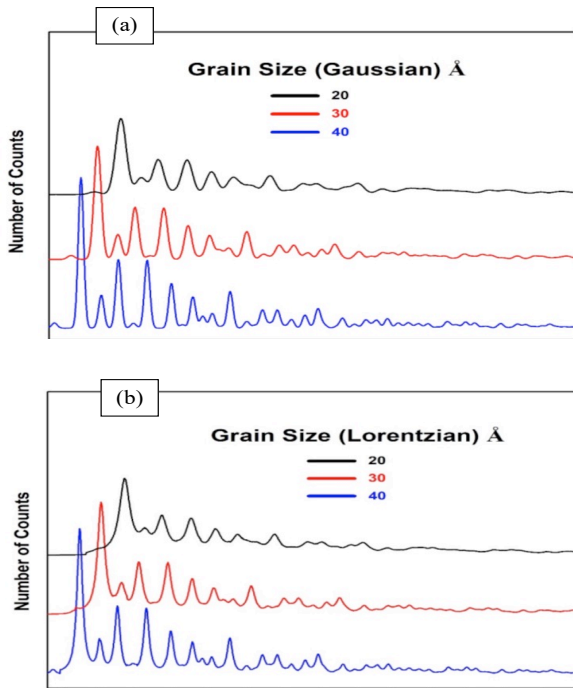


**Fig.9:** Effect of instrumental parameter on PDF plots.

**(b) Crystallite size:**

The values of the used crystallite size and the corresponding shape parameter at fixed wavelength and $Q_{max}$ are given in Table (5). The X-ray diffraction patterns for Gaussian and Lorentzian distribution are depicted in Figures (10) (a) and (b). The corresponding PDF plots are depicted in Figures (11) and (12). In both cases, diffraction peak broadening increases and, thus, the peak height decreases but without a shift in position. On the other hand, the PDF plot is greatly affected. Peak position and height are not affected but peak height decreases deistically (PDF peak cut-off) at r values nearly equal the crystallite size. So that, it seems that the PDF plot can be used as a rough estimation of the crystallite size as shown in Figures (11) and (12) and given by Page et al [18]. However, this direct information from the PDF should be taken carefully since it looks like the effect of increasing the broadening of X-ray diffraction peaks as shown in Figure (9). As the crystallite size increases, either Gaussian or Lorentzian, the quality of PDF plot is enhanced where the beak heights increases and resolution improved.

**Table 5:** Used values of crystallite size parameters (Gaussian and Lorentzian) at fixed wavelength and $Q_{max}$:

| λ (Å) | $Q_{max}$ (Å⁻¹) | Crystallite Size (Å) | Shape Parameter | |
|---|---|---|---|---|
| | | | Gaussian (IG) | Lorentzian (Y) |
| 0.3 | 0.7 | 20 | 0.738 | 0.859 |
| | | 30 | 0.328 | 0.573 |
| | | 40 | 0.185 | 0.429 |



**Fig.10:** Effect of crystallite size on XRD diffractograms for: (a) Gaussian distribution and (b) Lorentzian distribution.

**(c) Internal residual strain:**

Residual internal micro-strain for both Gaussian and Lorentzian distribution is defined as:

$$\text{Strain (Gaussian)} = (\pi/1.8)\ \sqrt{(u)}$$

and

$$\text{Strain (Lorentzian)} = (\pi/1.8)\ (x)$$

The values of the used residual strain and the corresponding shape parameter at fixed wavelength and $Q_{max}$ are given in Table (6). The corresponding diffraction patterns for Gaussian and Lorentzian distribution are depicted in Figures (13a) and (13b). The corresponding PDF for Gaussian and Lorentzian distribution are depicted in Figure (14) and Figure (15), respectively. In both cases broadening of diffraction peak increases without shift. On the other hand, the PDF plot is greatly affected at r-value >15Å., Generally, the peak height decreases and the peaks lose their sharpness as strain increases.

**ii- Diffraction peak intensity (number of counts):**

The diffraction patterns for different peak intensity (number of counts) are depicted in Figure (16) and the corresponding PDF plot is depicted in Figure (17). Consider the X-ray diffractograms, the peak positions and width do not change. At the same time no change in the PDF plots, either in the peak position or in the peak height (resolution). This is normal, where the PDF is used even for the non-crystalline (amorphous) materials and does not depend on the Bragg peaks.

**Table 6:** Used values of internal residual strain (Gaussian and Lorentzian) at fixed wavelength and Qmax:

| λ (Å) | $Q_{max}$ (Å⁻¹) | Strain (%) | Shape Parameter | |
|---|---|---|---|---|
| | | | Gaussian (u) | Lorentzian (x) |
| 0.3 | 0.7 | 1.00 | 0.003 | 0.057 |
| | | 10.0 | 0.013 | 0.115 |
| | | 20.0 | 0.029 | 0.172 |

### 3.1.3 Crystallographic Characteristics:

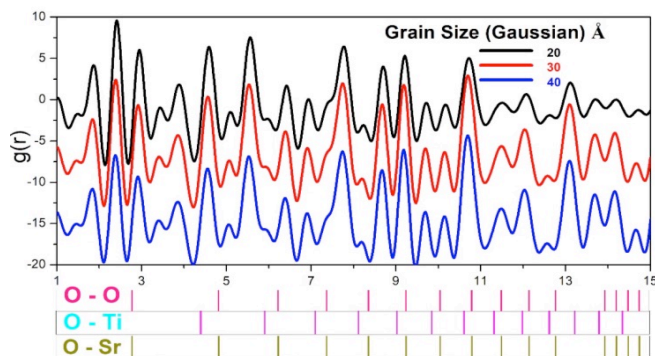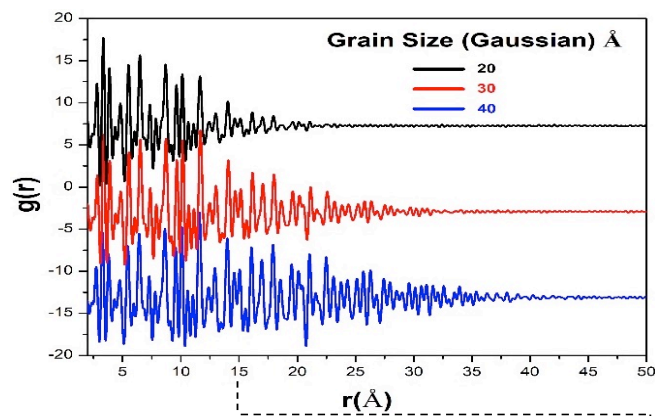**i- Errors in radial inter-atomic distances:**

The values of radial interatomic distances calculated from the structure characteristics of simulated parameters and those estimated (observed) from PDF as well as the errors in the observed redial distances are given in Table (7). The error did not exceed 10.0 % for inter-atomic radial distance longer than ≈ 2.0 Å, or 6.0 % for longer distances than ≈ 4.0 Å, which is accepted in structure refinement.

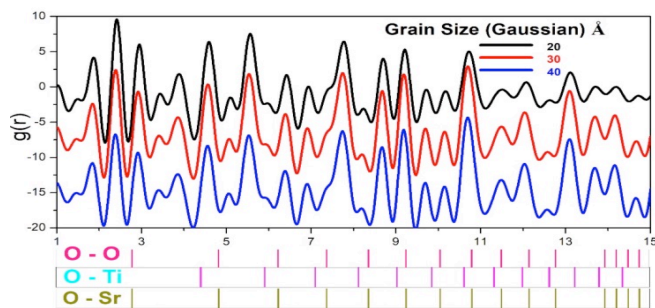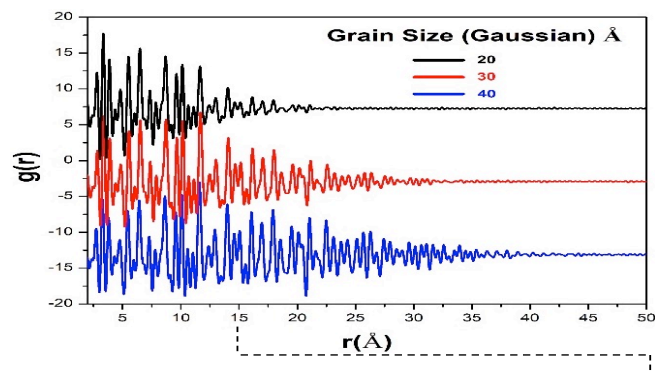**Table 7:** Redial distances from simulation and calculated PDF.

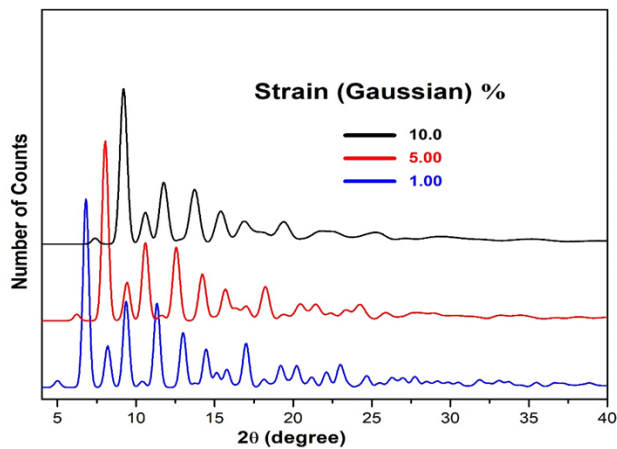| Inter-atomic type | Inter-atomic distance, r (Å) | | Error | |
|---|---|---|---|---|
| | Correct | Observed | Å | % |
| O1-O1 | 3.945 | 3.750 | 0.195 | 4.9 |
| O1-O2 | 2.789 | 2.690 | 0.099 | 3.5 |
| O-Ti | 1.973 | 1.680 | 0.293 | 14.8 |
| | 4.411 | 4.550 | 0.139 | 3.1 |
| | 5.917 | 5.607 | 0.310 | 5.2 |
| | 7.111 | 7.607 | 0.496 | 7.0 |
| O-Sr | 2.789 | 2.690 | 0.099 | 3.5 |
| | 4.831 | 4.550 | 0.281 | 5.8 |
| | 6.237 | 6.607 | 0.370 | 5.9 |
| | 7.380 | 7.607 | 0.227 | 3.1 |
| Ti-Ti Sr-Sr | 3.945 | 3.750 | 0.195 | 4.9 |
| | 5.579 | 5.607 | 0.028 | 0.5 |
| | 6.832 | 6.607 | 0.225 | 3.3 |
| | 7.890 | 7.607 | 0.283 | 3.6 |
| Ti-Sr | 3.410 | 3.750 | 0.340 | 10.0 |
| | 6.542 | 6.607 | 0.065 | 1.0 |





**Fig.11:** Effect of crystallite size for Gaussian distribution on PDF plots.





**Fig.12:** Effect of crystallite size for Lorentzian distribution on PDF plots.

**i- Tolerance of lattice Parameters:**

The second step in verification of the used program is to test the tolerance in the refinement of one of the crystallographic characteristics and lattice parameter is a simple one. The correct (actual) values as well as the started (wrong) values and the refined ones are given in Table (8). Every time the value of the lattice parameter is changed to smaller or larger than the correct value ($\pm$ 8.0 %), it comes back to the initial correct one. Thus, PDFgui program can be confidently used for structure refinement.

**Table 8:** Values of the refined lattice parameters (Å).

| Correct | Started | Refined |
|---------|---------|---------|
|         | 3.6     | 3.945   |
| 3.945   | 4.0     | 3.945   |
|         | 4.2     | 3.945   |





(a)



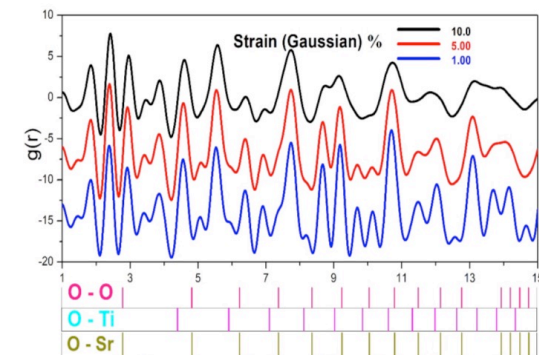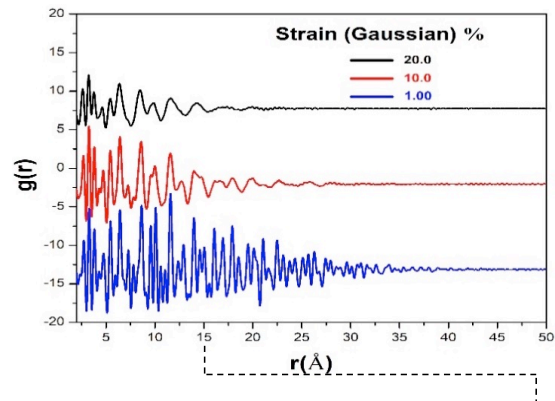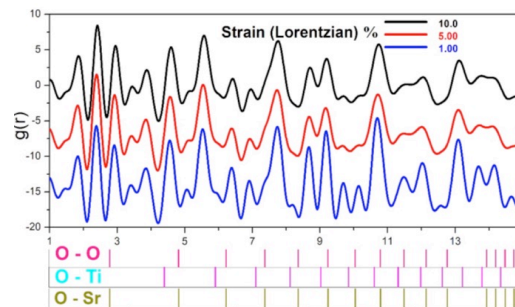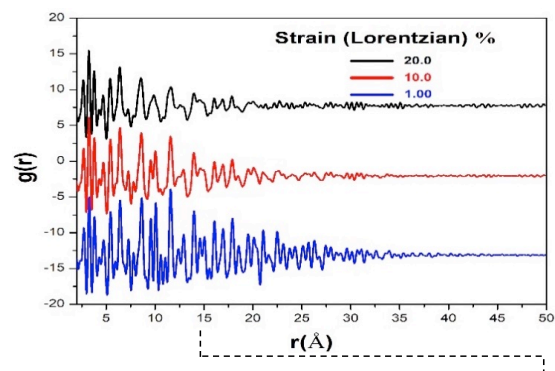**Fig.14:** Effect of residual strain for Gaussian distribution on PDF plots.



(b)

**Fig.13:** Effect of residual strain on X-ray diffraction patterns considering:

(a) Gaussian distribution and (b) lorentzian distribution.





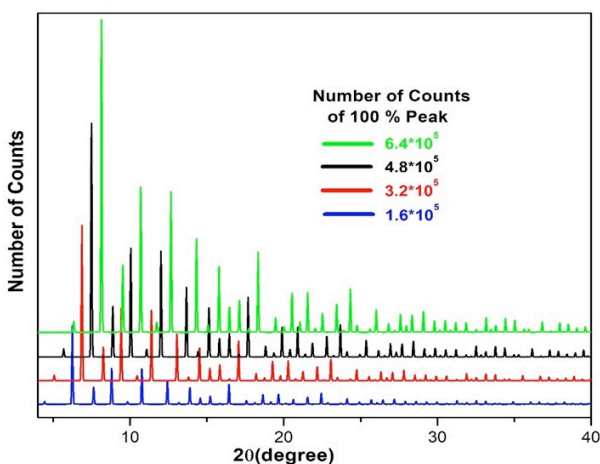**Fig.15:** Effect of residual strain for Lorentzian distribution on PDF plots.

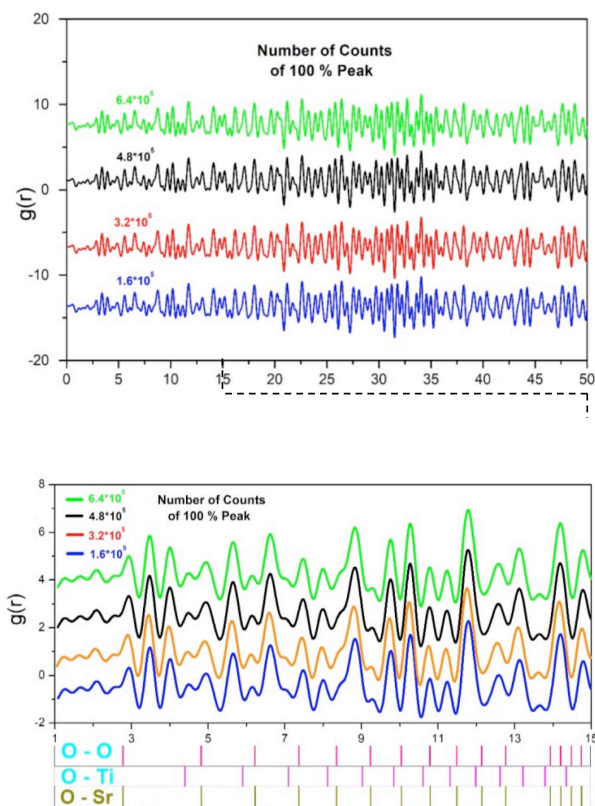**Fig.16:** Effect of number of counts on diffraction pattern.





**Fig.17:** Effect of number of counts on PDF plots.

## 4 Conclusions

According to the verification and individual investigation of the effect of data collection conditions and diffractogram characteristics on the quality of PDF plot, it is concluded, that:

1- Short wavelength is recommended where peaks become sharper and of higher intensity.
2- Large $Q_{max}$ is recommended from the point of views of both the diffractogram as well as the PDF plot. The number of diffraction peaks increases

and beaks in PDF plot become sharp and of higher intensity.

3- Step size ($\Delta 2\Theta$) does not affect the PDF plot.
4- As FWHM increases, peak heights (repels) in PDF decrease rapidly and disappear at smaller r-value. So, information on long range cannot be extracted. Therefore, it is recommended that the experimental conditions used for data collection should be specified to get sharp diffraction peaks (small broadening) as possible.
5- As the crystallite size decreases, peak position in PDF plot does not change but peak height decreases deistically (peak cut-off) at r-values nearly equal the crystallite size. So that, the PDF plot may be used carefully as a rough estimation of the crystallite size. Generally, as the crystallite size increases, either Gaussian or Lorentzian distribution, the quality of PDF plot is enhanced
6- As residual micro-strain increases, the PDF plot is greatly affected, where the peaks lose their sharpness, especially at r-vales longer than 15 Å, but still can be specified.
7- Peak intensity (number of counts) does not affect the PDF plots, either in the peak position or the peak height (resolution).
8- Direct space approach can be confidently used for structure refinement, where the error did not exceed 10.0 % for inter-atomic radial distance longer than $\approx$ 2.0 Å and 6.0 % for longer than $\approx$ 4.0 Å, which is accepted in structure refinement.
9- As tolerance is considered, every time the value of the lattice parameter is changed to smaller or larger than the correct value ($\pm$ 8.0 %), it comes back to the initial correct one. Thus, PDFgui program can be safely confidently used for structure refinement.
10- Although, advanced Synchrotron radiation shows better results, conventional X-ray source can be also used with accepted results.

## References

[1]    T. Egami and S. J. . Billinge, "Underneath the Bragg Peaks," *Mater. Today* **6**, 57 (2003).

[2]    R. Heimann, "X-Ray Powder Diffraction (XRPD)," in *Oxford Handb. Archaeol. Ceram. Anal.*, A. Hunt, Ed. (Oxford University Press, 2016).

[3]    W. I. F. David, K. Shankland, L. B. McCusker, and C. Baerlocher, *Structure Determination from Powder Diffraction Data*, in *Struct. Determ. from Powder Diffr. Data* **9780199205**, W. I. F. David, K. Shankland, L. B. McCusker, and C. Bärlocher, Eds. (Oxford University Press, 2006).

[4]    B. Shyam, K. H. Stone, R. Bassiri, M. M. Fejer, M. F. Toney, and A. Mehta, "Measurement and Modeling of Short and Medium Range Order in Amorphous Ta2O5 Thin Films," *Sci. Rep.* **6**, 32170 (2016).

[5] K. M. Ø. Jensen, A. B. Blichfeld, S. R. Bauers, S. R. Wood, E. Dooryhée, D. C. Johnson, B. B. Iversen, and S. J. L. Billinge, "Demonstration of thin film pair distribution function analysis (tfPDF) for the study of local structure in amorphous and crystalline thin films," *IUCrJ* **2**, 481–489 (2015).

[6] T. Proffen, "Analysis of disordered materials using total scattering and the atomic pair distribution function," in *Rev. Mineral. Geochemistry* **63** (2006).

[7] B. E. Warren, "X-ray determination of the structure of liquids and glass," *J. Appl. Phys.* **8**, 645–654 (1937).

[8] S. J. L. Billinge and M. G. Kanatzidis, "Beyond crystallography: The study of disorder, nanocrystallinity and crystallographically challenged materials with pair distribution functions," *Chem. Commun.* **4**, 749–760 (2004).

[9] N. Petkov, P. Birjukovs, R. Phelan, M. A. Morris, D. Erts, and J. D. Holmes, "Growth of ordered arrangements of one-dimensional germanium nanostructures with controllable crystallinities," *Chem. Mater.* **20**, 1902–1908 (2008).

[10] P. Juhás, T. Davis, C. L. Farrow, and S. J. L. Billinge, "PDFgetX3 : a rapid and highly automatable program for processing powder diffraction data into total scattering pair distribution functions," *J. Appl. Crystallogr.* **46**, 560–566 (2013).

[11] W. Kraus and G. Nolze, "POWDER CELL – a program for the representation and manipulation of crystal structures and calculation of the resulting X-ray powder patterns," *J. Appl. Crystallogr.* **29**, 301–303 (1996).

[12] J. Rodríguez-Carvajal, "Recent advances in magnetic structure determination by neutron powder diffraction," *Phys. B Condens. Matter* **192**, 55–69 (1993).

[13] L. Lutterotti, "Maud: a Rietveld analysis program designed for the internet and experiment integration," *Acta Crystallogr. Sect. A Found. Crystallogr.* **56**, s54–s54 (2000).

[14] V. Petkov, "RAD , a program for analysis of X-ray diffraction data from amorphous materials for personal computers," *J. Appl. Crystallogr.* **22**, 387–389 (1989).

[15] M. Wojdyr, "Fityk : a general-purpose peak fitting program," *J. Appl. Crystallogr.* **43**, 1126–1128 (2010).

[16] C. L. Farrow, P. Juhas, J. W. Liu, D. Bryndin, E. S. Božin, J. Bloch, T. Proffen, and S. J. L. Billinge, "PDFfit2 and PDFgui: computer programs for studying nanostructure in crystals," *J. Phys. Condens. Matter* **19**, 335219 (2007).

[17] A. Kinaci, C. Sevik, and T. Çağın, "Electronic transport properties of SrTiO3 and its alloys: Sr1−xLaxTiO3 and SrTi1−xMxO3 (M=Nb,Ta)," *Phys. Rev. B* **B82**, 155114 (2010).

[18] K. L. Page, T. Proffen, S. E. McLain, T. W. Darling, and J. A. TenCate, "Local atomic structure of Fontainebleau sandstone: Evidence for an amorphous phase?," *Geophys. Res. Lett.* **31**, 1–4 (2004).